

FAST COMMUNICATION

DIFFUSE INTERFACE ENERGIES CAPTURING THE EULER NUMBER: RELAXATION AND RENORMALIZATION*

QIANG DU[†], CHUN LIU[‡], ROLF RYHAM[§], AND XIAOQIANG WANG[¶]

Abstract. We introduce a set of new interfacial energies for approximating the Euler number of level surfaces in the phase field (diffuse-interface) representation. These new formulae have simpler forms than those studied earlier in [Q. Du, C. Liu and X. Wang, *Retrieving topological information for phase field models*, SIAM J. Appl. Math., 65, 1913-1932, 2005], and do not contain higher order derivatives of the phase field function. Theoretical justifications are provided via formal asymptotic analysis, and practical validations are performed through numerical experiments. Relaxation and renormalization schemes are also developed to improve the robustness of the new energy functionals.

Key words. Euler number, topological index, implicitly defined surfaces, phase field, diffuse interface, interfacial energy, surface tension, bending energy, vesicle membrane

AMS subject classifications. 57M50, 74A50, 74S99, 92C05

1. Introduction

The Euler number, or Euler-Poincaré index, is a topological index which can provide statistical information to classify types of surfaces and also be an indicator of critical topological events and possibly hysteresis in a dynamic process. When using the direct representation of surfaces, critical events, e.g., change of topology, are often associated with a singular transition, and thus necessitate re-meshing/reparametrization. Such singular transitions are difficult to treat. They require extensive computational efforts in doing detailed constructions, but more importantly, if dealt with in an ad hoc or artificial fashion, the correct physics or energetics may not even hold. Consequently, the detection and treatment of topological events present interesting and challenging problems that have been widely studied through various approaches [15, 17, 18, 21, 23, 24, 27]. There is also considerable interest in topological feature preservation in areas such as computer graphics and shape optimization [1, 14, 16, 26].

In contrast to most direct methods, the phase field (or diffuse interface) model uses an implicitly defined interface representation which is indifferent to most topological changes [2, 3, 4, 5, 6, 19]. A change of the topology is in general not detectable by changes in the surface or mean curvature energy [11]. Hence it is desirable to introduce a new interfacial energy which can provide statistics on the interface topology.

In this paper we study approximations of the Euler number of an interface Γ , which is implicitly defined by the zero level set of a phase field function ϕ defined in

*Received: September 29, 2006; accepted (in revised version): January 11, 2007. Communicated by Peter Smereka.

[†]Department of Mathematics, Pennsylvania State University, University Park, PA 16802, USA (qdu@math.psu.edu).

The research is supported in part by NSF-DMS 0409297, NSF-DMR 0205232 and NSF-CCF 0430349.

[‡]Department of Mathematics, Pennsylvania State University, University Park, PA 16802, USA (liu@math.psu.edu).

The research is supported in part by NSF-DMS 0405850 and NSF-DMS 0509094.

[§]Department of Mathematics, Rice University, Houston, TX 77005, USA (ryham@rice.edu).

[¶]School of Computational Science and Department of Mathematics, Florida State University, Tallahassee, FL 32306, USA (xwang@scs.fsu.edu).

a computational domain $\Omega \subset \mathbb{R}^3$, by functionals of the following form:

$$\frac{\chi_\epsilon(\phi)}{2} = -\frac{1}{4\pi c_0 \epsilon} \int_{\Omega} \left(\Delta \phi - \frac{1}{\epsilon^2} W'(\phi) \right) p(\phi) dx. \quad (1.1)$$

For the remainder of this paper we assume that W is the double well potential, $W(t) = (t^2 - 1)^2/4$, but more general W may also be applicable. The constant c_0 is a normalization parameter, depending on W and p , as specified later. In this work we study χ_ϵ for p of the form $p(t) = d((1 - t^2)^n)/dt = -2n(1 - t^2)^{n-1}t$ for $n \geq 1$.

In [11], several formulae for the computation of the Euler number were introduced in the phase field context. For instance,

$$\frac{\chi_o(\phi)}{2} = \frac{1}{4\pi c} \int_{\Omega_c} \left[\frac{1}{|\nabla \phi|} \Lambda \left(\nabla^2 \phi - \frac{\nabla \phi \cdot \nabla^2 \phi \cdot \nabla \phi}{|\nabla \phi|^4} \nabla \phi \otimes \nabla \phi \right) \right] dx \quad (1.2)$$

where the subscript o is used to denote the old definition, $\Lambda(M)$ is the sum of the determinant of the three principal minors of a 3 by 3 matrix M and c is a constant explicitly given based on the computational domain Ω_c . The authors also studied several simplified forms under a special ansatz and a simple approximation of the index of curves in two dimensional space, which are related to the functional (1.1) considered in this paper with $p(t) = 1$.

Some advantages of the new interfacial energy are: (1.1) is relatively easy to compute while (1.2) requires the evaluation of the Hessian matrix containing second order derivatives, and (1.1) effectively avoids using high order derivative terms after an integration by part on the term $\Delta \phi$. In addition, (1.1) is well defined for $\phi \in H^2(\Omega)$ while (1.2) is not in general. Moreover, its variational derivative, in weak form,

$$(\chi'_\epsilon(\phi), v) = -\frac{1}{\pi c_0 \epsilon} \int_{\Omega} \left(p'(\phi) \nabla \phi \nabla v + \frac{1}{2} |\nabla \phi|^2 p''(\phi) v + \frac{1}{2\epsilon^2} \partial_\phi (W'(\phi) p(\phi)) v \right) dx,$$

contains differentiations of order less than two. It thus becomes feasible that (1.1) may be used as constraints for schemes where the energy functional provides control on the higher order space derivatives, like those found in the Cahn-Hilliard formulation or approximations of elastica [20, 22].

This paper is divided as follows: In section 2, we give the preliminary derivation of the new phase field energy for approximating the Euler number. In section 3, we present some numerical simulation for a class of phase field functions where the new formula (1.1) is in good agreement with the actual Euler number. In section 4, through comparisons of the numerical simulations obtained with different formulae, we develop some relaxation and renormalization procedures for the accurate approximation of the Euler number with the new formulae in more general cases. We also provide some formal justification to the relaxation procedure. Finally, we end the paper with some conclusions in section 5.

2. Simple approximation of the Euler number

In this section, we validate (1.1) for a restricted class of phase field functions ϕ_ϵ . First we recall some basic geometric identities in terms of the signed distance function d . Let $\Gamma \subset \Omega$ be a smooth, embedded surface without boundary and $d(x) = |\text{dist}(x, \Gamma)|$ if x lies outside of the region enclosed by Γ and $d(x) = -|\text{dist}(x, \Gamma)|$ otherwise. The function d is smooth in some neighborhood of Γ wherein d satisfies $|\nabla d| = 1$ and $0 = \nabla \cdot (\nabla^2 d \nabla d) = \nabla d \cdot \nabla \Delta d + \text{tr}((\nabla^2 d)^2)$. It is clear that $\nabla d(z)$ is the outward pointing unit normal \mathbf{n} of Γ and it is easy to check that $\Delta d(z) = \text{tr}(\nabla^2 d) = 2H$ where H is the

mean curvature. The matrix $\nabla^2 d$ has three eigenvalues 0, k_1 and k_2 where $H = (k_1 + k_2)/2$ and $K = k_1 k_2$. The new energy (1.1) relies on the following observation

$$\begin{aligned} 2K &= 2k_1 k_2 = (k_1 + k_2)^2 - (k_1^2 + k_2^2) \\ &= (\Delta d)^2 - \text{tr}((\nabla^2 d)^2) = (\Delta d)^2 + \nabla d \cdot \nabla \Delta d \\ &= \nabla \cdot (\nabla d \Delta d). \end{aligned} \tag{2.1}$$

Suppose that the phase field function takes the form of a particular one dimensional profile in the direction normal to the surface: $\phi_\epsilon = q(d/\epsilon)$ where $q(t) = \tanh(t/\sqrt{2})$. Let $P(t) = (1 - t^2)^n$ so that $p(t) = dP(t)/dt$ and define

$$c_0 = 2 \int_{-\infty}^{\infty} P(q(s)) ds. \tag{2.2}$$

Using integration by parts, the co-area formula [13], and identities $|\nabla d| = 1$ and (2.1), we get as ϵ converges to 0 that

$$\begin{aligned} \frac{\chi_\epsilon(\phi_\epsilon)}{2} &= -\frac{1}{4\pi c_0 \epsilon} \int_{\Omega} \left(\Delta \phi - \frac{1}{\epsilon^2} W'(\phi) \right) p(\phi) dx = -\frac{1}{4\pi c_0 \epsilon^2} \int_{\Omega} q'(d/\epsilon) \Delta d p(q(d/\epsilon)) dx \\ &= -\frac{1}{4\pi c_0 \epsilon} \int_{\Omega} \Delta d \nabla d \cdot \nabla P(q(d/\epsilon)) dx = \frac{1}{4\pi c_0 \epsilon} \int_{\Omega} \nabla \cdot (\nabla d \Delta d) P(q(d/\epsilon)) dx \\ &= \frac{1}{4\pi c_0 \epsilon} \int_{-\infty}^{\infty} P(q(r/\epsilon)) \int_{\{d=r\}} \nabla \cdot (\nabla d \Delta d) dS dr \rightarrow \frac{1}{4\pi} \int_{\Gamma} K dS = \frac{\chi(\Gamma)}{2}. \end{aligned}$$

Note that the $\chi(\Gamma)/2$ given here is actually half of the conventional Euler number $\chi(\Gamma)$ of a surface defined in standard texts. For convenience and easy comparison with an earlier work [11], this convention is made throughout the present paper and the readers are reminded of this obvious difference. Without loss of generality, we also assume here that the signed distance function is smooth in all of Ω (else, we may consider a modified distance function which is smooth and takes a constant value $\delta/2$ outside some δ -neighborhood of Γ). The limit in the above relation follows from elementary properties of the tanh function.

We have derived the Euler number formula under the pretext that ϕ enjoys a restrictive structural assumption. However, there are cases, such as in the leftmost graph of figure 4.2, where the formula (1.1) grossly over-estimates the Euler number and the structural assumption no longer holds. The relaxation and renormalization procedures devised in section 4 are aimed at partially amending this problem.

3. Preliminary numerical experiments

First we present some numerical experiments using our new Euler number functional for $p(t) = 4(t^2 - 1)t$ and $c_0 = 8\sqrt{2}/3$. The three-dimensional numerical experiments are performed in a computational domain $[-\pi, \pi]^3$. For the spatial discretization, a Fourier spectral method is used with a $64 \times 64 \times 64$ mesh unless otherwise noted. Mesh refinements are often performed to ensure the accuracy of the numerical results.

In our first experiment, we validate (1.1) for ϕ which takes exactly the hyperbolic tangent profile normal to a surface. Consider the cases of a sphere and a torus, we take the parameter values $\epsilon = 1.768h = 0.17355$ so that enough resolution of the phase field profile is assured. We let $\phi(x) = \tanh((0.65\pi - |x|)/(\sqrt{2}\epsilon))$ for a sphere of radius $r = 0.65\pi$, while for the torus, we let $\phi(x) = \tanh((0.25\pi - [(x_1 - 0.5\pi \cos\theta)^2 + (x_2 -$

TABLE 3.1. Numerically computed Euler number.

| Shape \ Formula | New formula (1.1) | Old formula (1.2) |
|-----------------|-------------------|-------------------|
| Sphere | 1.0000 | 0.9995 |
| Torus | 0.0003 | 0.0112 |

$0.5\pi \sin\theta)^2 + x_3^2]^{1/2}/(\sqrt{2}\epsilon)$ where $\theta = \cos^{-1}(x_1/|x|)$. Table 3 gives the Euler numbers $\chi_\epsilon(\phi_\epsilon)/2$ calculated by formulae (1.1) and (1.2) respectively, note again that the values computed are approximations of $\chi(\Gamma)/2$ which are just half of the conventional Euler number values for surfaces (e.g., $\chi(\Gamma) = 2$ for a sphere, and $\chi(\Gamma)/2$ matches with the values for the sphere in the table and in the plots). From the data, it is obvious that both formulae give relatively good approximations.

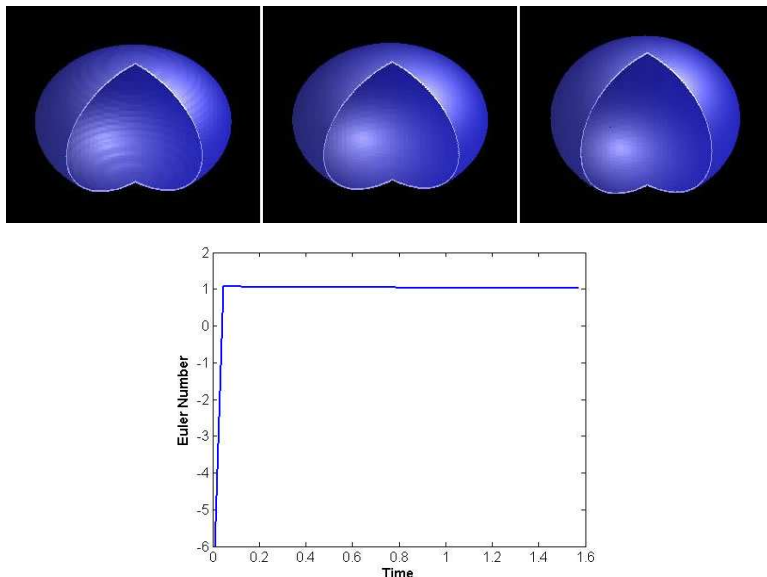


FIG. 3.1. Vesicle deformation and its Euler number calculated by (1.1) at different times.

In our second experiment, we consider the surface obtained from the minimization of the energy

$$H_\epsilon(\phi) = \int_{\Omega} \frac{\epsilon}{2} \left(\Delta\phi - \frac{1}{\epsilon^2}(\phi^2 - 1)\phi \right)^2 dx, \quad (3.1)$$

which models the deformation of vesicle membrane configurations minimizing their bending energy H_ϵ [10]. The variational problem is also related to a functional introduced by De Giorgi which has recently attracted much attention [20, 22].

The dynamic deformation process is simulated via a gradient flow of the energy H_ϵ [12], subject to the constraint with a constant surface area (which is related to a functional like (4.5) in the phase field description). In the experiment, as shown in Fig. 3.1, an initial ellipsoid shape gradually deforms to a sphere. The Euler numbers, again referring to $\chi_\epsilon(\phi_\epsilon)/2$ as calculated by formula (1.1), are plotted in Fig. 3.1 with respect to time. The calculated result lacks accuracy initially, however, soon after

a transient period, the computed values of $\chi_\epsilon(\phi_\epsilon)/2$ from (1.1) converge to 1.0 very quickly.

4. Relaxation and renormalization

In some cases, the functional (1.1) does not poorly approximates well the Euler number of the implicitly defined interface (see for example figure 4.2.) This section is devoted to addressing this problem. First we introduce an artificial relaxation scheme using the energy (3.1). Then we apply a renormalization of the phase field by choosing n large in the weighting function $p(t) = -2n(1 - t^2)^{n-1}t$. Some formal asymptotic analysis is given to motivate the artificial relaxation scheme and its connection with the optimal profile used to derive (1.1) in section 2.

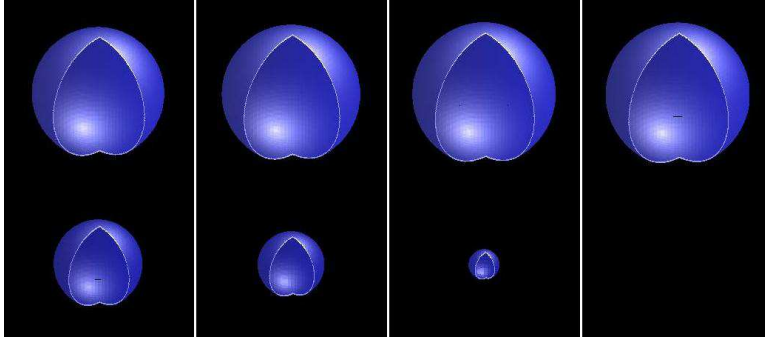


FIG. 4.1. Deformation of two bubbles: Larger bubble absorbs the smaller one.

We describe the relaxation scheme by an example from the general framework of an incompressible fluid/phase field coupling (see [9], for instance.) Let $E = E(\phi) \geq 0$ be an arbitrary energy functional and consider

$$\mathbf{u}_t + \mathbf{u} \cdot \nabla \mathbf{u} + \nabla p = \nu \Delta \mathbf{u} + E'(\phi) \nabla \phi, \tag{4.1}$$

$$\nabla \cdot \mathbf{u} = 0, \tag{4.2}$$

$$\phi_t + \mathbf{u} \cdot \nabla \phi = -\gamma E'(\phi). \tag{4.3}$$

Here $'$ denotes the Euler-Lagrange variational derivative, i.e., for $v \in C_0^\infty(\Omega)$, we have $(E'(\phi), v) = \frac{d}{dt} E(\phi + tv)|_{t=0}$. The above system models the two phase flow of an incompressible fluid which has an interfacial energy $E = E(\phi)$ associated with the two phases, e.g., the surface area of the interface. Our relaxation scheme replaces the energy E by the perturbed energy

$$E_\lambda(\phi) = E(\phi) + \lambda H_\epsilon(\phi), \tag{4.4}$$

where H_ϵ is defined in (3.1). We point out that there are three artificial parameters to regularize the system, namely, the parameter ϵ which regularizes the sharp interface formulation, the parameter λ which introduces higher order energy contribution; and the parameter γ which regularizes the transport problem by introducing additional dissipation. Replacing E by the perturbed energy E_λ in (4.1) and (4.3), we get the following energy dissipation law

$$\frac{d}{dt} \left(\frac{1}{2} \|\mathbf{u}\|^2 + E_\lambda(\phi) \right) = -\nu \|\nabla \mathbf{u}\|^2 - \gamma \|E'_\lambda(\phi)\|^2 \leq 0.$$

If the initial data are chosen so that $E_\lambda(\phi_0)$ and $\|\mathbf{u}\|_{L^2(\Omega)}^2$ are bounded by some constant M independently of ϵ , then $H_\epsilon(\phi)$ remains bounded independently of ϵ for all later times as well. More discussions on the well-posedness of the resulting system involving the bending energy H_ϵ can be found in [7]. Taking λ to zero, the above system ideally returns to the original coupling only involving E .

We now consider an example, as shown in Fig. 4.1, that demonstrates the hydrodynamic evolution of the coarsening of two bubbles governed by (4.1-4.3), where E is replaced by the perturbed energy (4.4) with

$$E(\phi) = \int_{\Omega} \left(\frac{\epsilon}{2} |\nabla \phi|^2 + \frac{1}{\epsilon} W(\phi) \right) dx. \quad (4.5)$$

The computation is again performed by the Fourier spectral method with a $64 \times 64 \times 128$ grid which offers sufficient resolution. The domain is $[-\pi, \pi] \times [-\pi, \pi] \times [-2\pi, 2\pi]$. The volume of all the bubbles is preserved by taking the integral of ϕ to be -419.5 at all time. The initial surface area, evaluated via (4.5), is chosen to be 61.2. For detailed numerical procedures, we refer to [12].

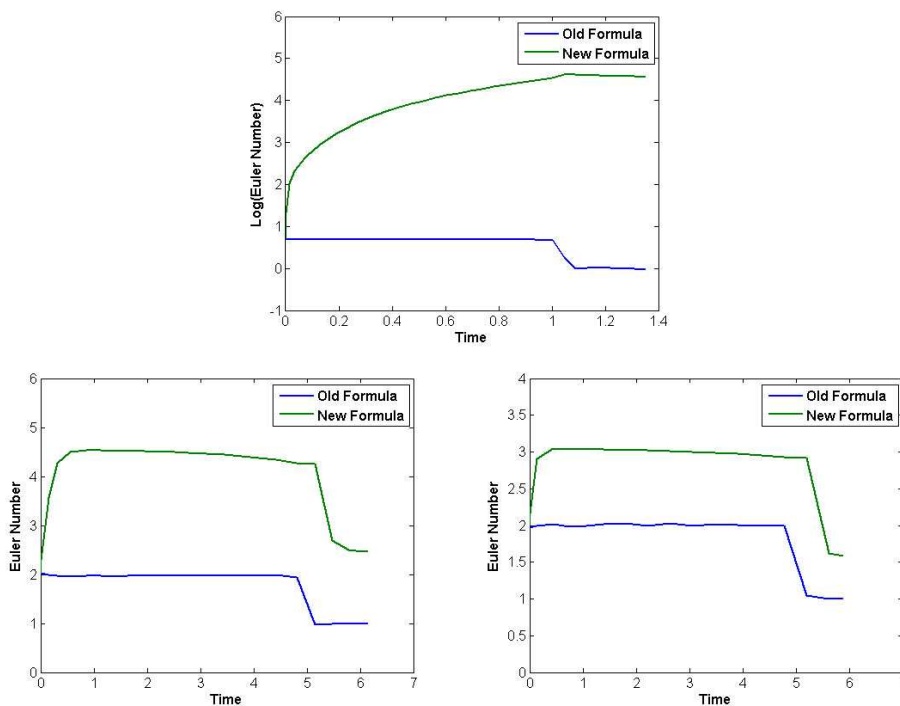


FIG. 4.2. Comparison of Euler number computation using the old formula (1.2) and new formula (1.1), with $\lambda=0, 0.1$ and 0.2 .

Unlike the experiments in section 3, the new formula (1.1) with $p(t) = 4(t^2 - 1)t$ and $c_0 = 8\sqrt{2}/3$ does not give satisfactory results in the absence of relaxation ($\lambda = 0$). In fact, it tends to over-estimate the Euler number. By increasing λ , the results seem to improve (see Fig. 4.2).

A closer look at the example reveals that during the deformation of the bubbles, even with the relaxation, which confines the distortion of the profile of the phase

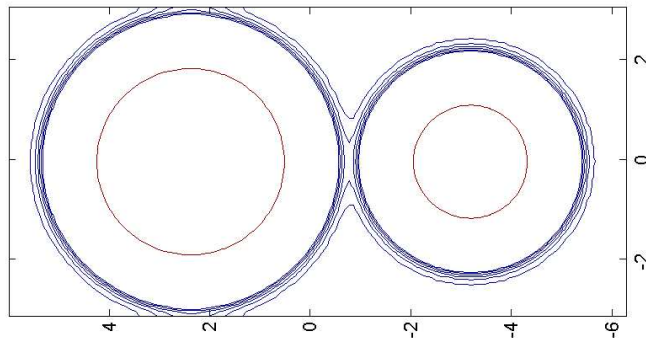


FIG. 4.3. Contour of the phase field ϕ at $t=1.13$.

function ϕ near the interface, the new Euler number formula remains sensitive to the small distortion away from the interface which is the cause of inaccuracy in the above example, as illustrated in the contour plot in Fig. 4.3 of the phase field function (at time $t=1.13$ and $\lambda=0.1$). The contours lines are drawn for values in between -1 and -0.993 with an increment of 5.0×10^{-5} , and the two well-separated red curves give the zero level set of ϕ . The plot reveals a connected contour structure away from the interface.

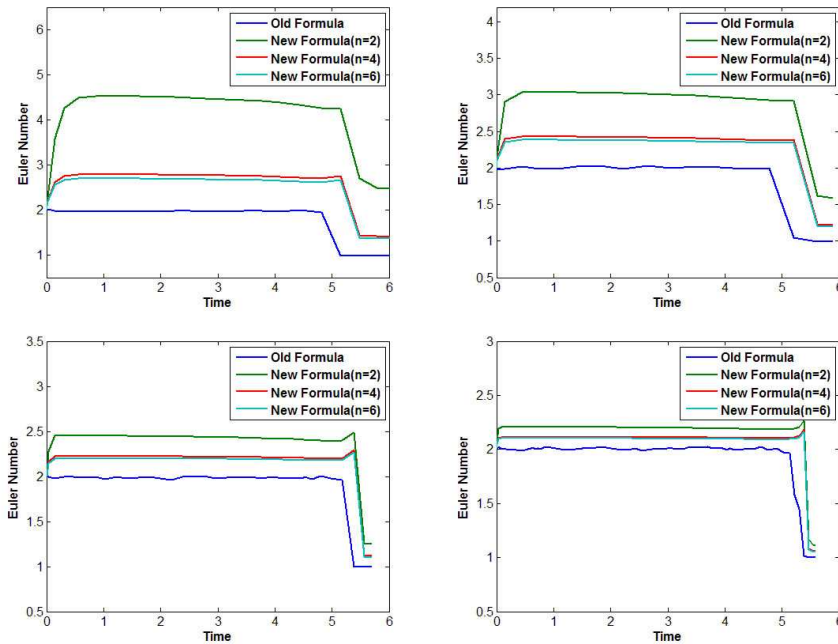


FIG. 4.4. The improvement of $\chi_\epsilon(\phi_\epsilon)/2$ due to the combination of relaxation and renormalization: λ is taken to be 0.1, 0.2, 0.4 and 0.8, with each plot showing results for $n=2, 4$ and 6.

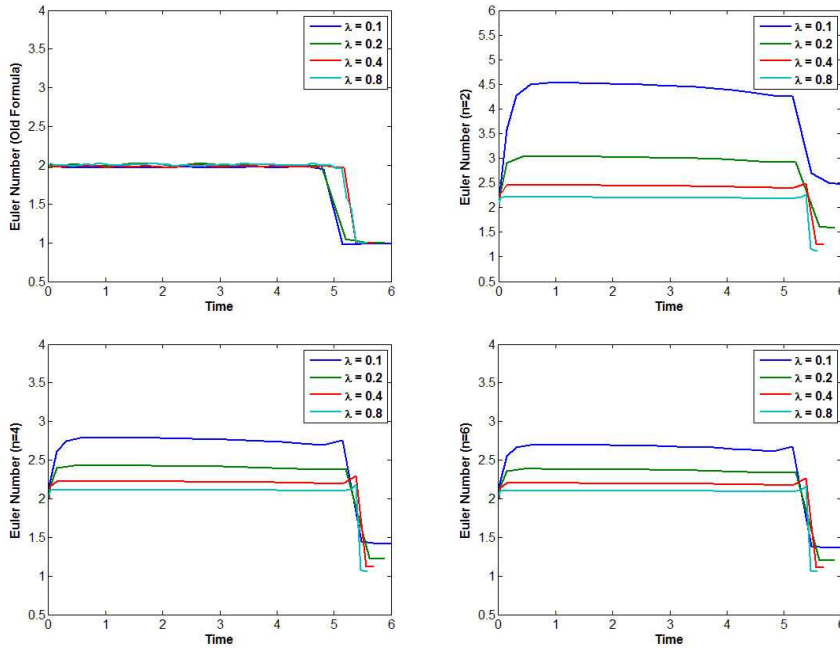


FIG. 4.5. The improvement of $\chi_\epsilon(\phi_\epsilon)/2$ due to the combination of relaxation and renormalization: computed Euler number from the old formula (1.2) and from (1.1) with n being 2, 4 and 6, with each plot showing results for $\lambda=0.1, 0.2, 0.4$ and 0.8.

In order to compensate for the sensitivity displayed in the above study, we introduce a renormalization of the Euler number formula. Here, we study the cases $p(t) = -2n(1-t^2)^{n-1}t$ for $n=2, 4$ and 6 where $c_0 = 8\sqrt{2}/3, 64\sqrt{2}/35$ and $1024\sqrt{2}/693$ respectively. For large n , the extra factor $(1-\phi^2)^{n-1}$ removes the contribution away from the interface where ϕ is typically close to ± 1 .

The numerical results of $\chi_\epsilon(\phi_\epsilon)/2$ given in Fig. 4.4 and Fig. 4.5 illustrate the effect of the relaxation and renormalization in the calculation of the Euler number by the new diffuse interface energies. A comparison with the results computed via the old formula (1.2) is also provided which again illustrates the robustness and accuracy of the latter. But as explained before, it is advantageous to employ the newer and simpler energies developed in this paper for many applications, such as for topology control purposes. Our experiments show that combining both the λ -relaxation and the n -renormalization is a very effective approach and it leads to significantly more accurate results under the new formulation.

We now briefly discuss why the introduction of the particular relaxation energy (3.1) via (4.4) possibly improves the approximation by the Euler number formula. Recall that in the derivation/validation of (1.1) (section 2), the phase fields are limited to those profiles satisfying $\phi(x) = \tanh(d(x)/(\sqrt{2}\epsilon))$. More generally, the phase field profile may satisfy the ansatz $\phi(x) = q(d(x)/\epsilon) + \epsilon h(x) + O(\epsilon^2)$ for some arbitrary profile q and for some well-behaved function h . For fixed λ , the relaxation scheme guarantees that $H_\epsilon(\phi)$ is bounded independently of ϵ . This, in combination with the ansatz, implies that $q(t) \equiv \tanh(t/\sqrt{2})$ and $h \equiv 0$. To see this, we may simply expand $H_\epsilon(\phi)$ in ϵ or refer to the calculation given in [8, 25]. The uniform H_ϵ bound tends to

enforce an optimal profile for the phase field, thereby leading to the accuracy of the approximation $\chi_\epsilon(\phi)$.

Finally, we want to point out the limitation and validity of the above approximation/regularization. Although the relaxation using the bending (Willmore) energy (3.1) does provide better control of the profile across the transition layer (hence assuring a more accurate Euler number calculation), it may well change the original dynamical problem. For instance, the presence of the bending energy may alter the interaction mechanism of the interface and flow fields, especially when the interface has regions of large curvature. Again, we elaborate that the key point of this paper is to introduce a simpler formula to compute the Euler number which relies more significantly on the profile of the transition layer. The relaxation and renormalization may be seen as ways to capture the Euler number but we do not at all claim these are optimal or even necessary. We are investigating more robust methods for maintaining the optimal profile and calculating the Euler number.

5. Conclusion

In summary, built upon earlier works on phase field membrane modelling, we developed a few new formulations of interfacial energies for estimating the Euler number of a free surface described by a phase field function. While in the previous work [11], we have sought a formula with more generality, the emphasis here is to look for more specialized but still effective formulae. The new energy given here is simpler and of a more attractive form. It does not need to involve high order derivatives and thus is more suitable to be used as a control and/or constraint in various applications. The simplifications are made possible by exploring the special optimal profile structures of phase field models, which may be induced by energy relaxation. The numerical experiments show that the new formula can be successfully implemented to retrieve topological information.

Of course, the Euler number alone does not determine completely the topology of an interface. Further studies on computing other topological indices as well as more extensive numerical experiments will be carried out in the future.

Acknowledgment. The authors would like to thank the referee for providing helpful comments on the paper.

REFERENCES

- [1] O. Alexandrov and F. Santosa, *A topology-preserving level set method for shape optimization*, J. Comput. Phys., 204, 121-130, 2005.
- [2] D. Anderson, G. McFadden and A. Wheeler, *Diffuse-interface methods in fluid mechanics*, Annual review of fluid mechanics, 30, 139-165, 1998.
- [3] G. Caginalp and X. Chen, *Phase field equations in the singular limit of sharp interface problems*, On the Evolution of Phase Boundaries, Springer, New York, 1-27, 1992.
- [4] J. W. Cahn and J. E. Hillard, *Free energy of a nonuniform system.I. Interfacial free energy*, J. Chem. Phys., 28, 258-267, 1958.
- [5] T. F. Chan, S. H. Kang and J. H. Shen, *Euler's elastica and curvature-based inpainting*, SIAM J. Appl. Math., 63, 564-592, 2002.
- [6] L. Q. Chen, *Phase-field models for microstructure evolution*, Annual Review of Materials Science, 32, 113-140, 2002.
- [7] Q. Du, M. Li and C. Liu, *Analysis of a phase field Navier-Stokes vesicle-fluid interaction model*, Disc. Cont. Dyn. Sys. B., to appear.
- [8] Q. Du, C. Liu, R. Ryham and X. Wang, *A phase field formulation of the Willmore problem*, Nonlinearity, 18, 1249-1267, 2005.
- [9] Q. Du, C. Liu, R. Ryham and X. Wang, *Modeling vesicle deformations in flow fields via energetic variational approaches*, preprint, 2006.

- [10] Q. Du, C. Liu and X. Wang, *A phase field approach in the numerical study of the elastic bending energy for vesicle membranes*, J. Comp. Phys., 198, 450-468, 2004
- [11] Q. Du, C. Liu and X. Wang, *Retrieving topological information for phase field models*, SIAM J. Appl. Math., 65, 1913-1932, 2005.
- [12] Q. Du, C. Liu and X. Wang, *Simulating the deformation of vesicle membranes under elastic bending energy in three dimensions*, J. Comp. Phys., 212, 757-777, 2005.
- [13] L. Evans and R. Gariepy, *Measure Theory and Fine Properties of Functions*, Studies in Advanced Mathematics, CRC Press, Boca Raton 1992.
- [14] H. Edelsbrunner, D. Letscher and A. Zomorodian, *Topological persistence and simplification*, Discrete and Computational Geometry, 28, 511-533, 2002.
- [15] J. Glimm, J. Grove, X. Li and D. Tan, *Robust computational algorithms for dynamic interface tracking in three dimensions*, SIAM J. Sci. Comp., 21, 2240-2256, 2000.
- [16] X. Han, C. Xu and J. Prince, *A topology preserving level set method for geometric deformable models*, IEEE Trac. Pattern Anal. Mach. Intelligence, 25, 755-768, 2003.
- [17] D. Juric and G. Tryggvason, *Computations of boiling flows*, Int. J. Multiphase Flow, 24, 387-410, 1998.
- [18] J. Lowengrub and L. Truskinovsky, *Quasi-incompressible Cahn-Hilliard fluids and topological transitions*, R. Soc. Lond. Proc. Ser. A Math. Phys. Eng. Sci., 454, 2617-2654, 1998.
- [19] L. Modica and S. Mortola, *Il limite nella Γ -convergenza di una famiglia di funzionali ellittici*, (Italian) Boll. Un. Mat. Ital. A(5), 14, 3, 526-529, 1977.
- [20] R. Moser, *A higher order asymptotic problem related to phase transitions*, SIAM J. Math. Anal., 37, 712-736, 2005.
- [21] J. A. Sethian, *Level Set Methods and Fast Marching Methods: evolving interfaces in computational geometry, fluid mechanics, computer vision, and materials science*, Cambridge University Press, New York, 2nd edition, 1999.
- [22] M. Röger and R. Schatzle, *On a modified conjecture of De Giorgi*, preprint, 2006.
- [23] M. Sussman, P. Smerka and S. Osher, *A level set approach for computing solutions to incompressible two-phase flow*, J. Comp. Phys., 114, 146-159, 1994.
- [24] D. Torres and J. Brackbill, *The point-set method: Front-tracking without connectivity*, J. Comput. Phys., 165, 620-644, 2000.
- [25] X. Wang, *Asymptotic analysis of phase field formulations of bending elasticity models*, preprint, 2006.
- [26] Z. Wood, H. Hoppe, M. Desbrun and P. Schroder, *Removing excess topology from isosurfaces*, ACM Transactions on Graphics, 23, 190-208, 2004.
- [27] H.-K. Zhao, T. Chan, B. Merriman and S. Osher, *A variational level set approach to multiphase motion*, J. Comput. Phys., 127, 179-195, 1996.